BIOCHEMISTRY
including biophysical chemistry & molecular biology

Article

pubs.acs.org/biochemistry

Designed Hairpin Peptides Interfere with Amyloidogenesis Pathways: Fibril Formation and Cytotoxicity Inhibition, Interception of the Preamyloid State

Kelly N. L. Huggins,[†] Marco Bisaglia,[‡] Luigi Bubacco,[‡] Marianna Tatarek-Nossol,[§,∥] Aphrodite Kapurniotu,[∥] and Niels H. Andersen*,[†]

[†]Department of Chemistry, University of Washington, Seattle, Washington 98195, United States

[‡]Department of Biology, University of Padova, Padova 35121, Italy

[§]Department of Biochemistry and Molecular Cell Biology, RWTH Aachen University, Aachen D-52074, Germany

[∥]Division of Peptide Biochemistry, Technische Universität München, Freising D-85354, Germany

Supporting Information

ABSTRACT: Hairpin peptides bearing cross-strand Trp-Trp and Tyr-Tyr pairs at non-H-bonded strand sites modulate the aggregation of two unrelated amyloidogenic systems, human pancreatic amylin (hAM) and α-synuclein (α-syn), associated with type II diabetes and Parkinson's disease, respectively. In the case of hAM, we have previously reported that inhibition of amyloidogenesis is observed as an increase in the lag time to amyloid formation and a diminished thioflavin (ThT) fluorescence response. In this study, a reduced level of hAM fibril formation is confirmed by transmission electron microscopy imaging. Several of the hairpins tested were significantly more effective inhibitors than rat amylin. Moreover, a marked inhibitory effect on hAM-associated cytotoxicity by the more potent hairpin peptide is demonstrated. In the case of α-syn, the dominant effect of active hairpins was, besides a weakened ThT fluorescence response, the earlier appearance of insoluble aggregates that do not display amyloid characteristics with the few fibrils observed having abnormal morphology. We attribute the alteration of the α-synuclein aggregation pathway observed to the capture of a preamyloid state and diversion to nonamyloidogenic aggregates. These β-hairpins represent a new class of amyloid inhibitors that bear no sequence similarity to the amyloid-producing polypeptides that are inhibited. A mechanistic rationale for these effects is proposed.

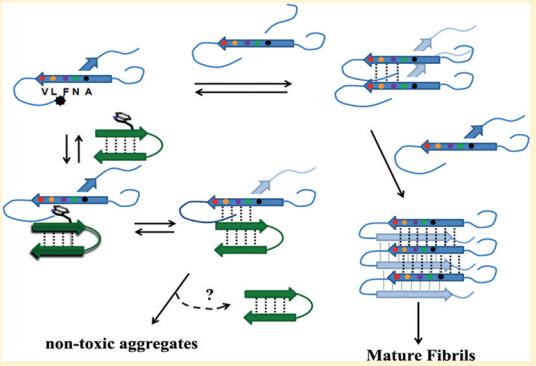

Protein folding diseases are an area of intense interest at present. Many protein folding diseases involve the formation of polypeptide aggregate deposits with a common cross-β-sheet fibrillar geometry and dye staining properties. Such amyloid fibrils are associated with more than 40 human diseases and conditions,[1] including type II diabetes,[2] Parkinson's disease (PD) (α-synuclein aggregates in Lewy bodies),[3] and other neurodegenerative conditions (e.g., Alzheimer's and Huntington's diseases). Fibril formation kinetics[4,5] imply a complex multistage, autocatalytic nucleation-dependent polymerization process with a lag phase followed by rapid, cooperative fibril formation.

While there are many therapeutic strategies[6,7] for amyloid-associated diseases, there is a commonly held expectation that amyloidogenesis inhibition has potential as either a preventative or ameliorating therapy for some of these medical conditions that cause human suffering and exact a tremendous societal burden. Three strategies related to the amyloidogenesis process are given here: (1) interfering with the processing of the proteins that afford the amyloidogenic peptides, (2) diverting preamyloid intermediates prior to the toxic states to nontoxic aggregates, and (3) reducing the steady-state concentration of toxic intermediates[8,9] in the amyloidogenic pathway by tinkering with the relative rates of the steps in the aggregation pathway. Therapeutic development based on the third strategy requires greater definition of the mechanisms of amyloidogenesis and the identification of the toxic species for each of the disease-related amyloidogenic species. Selective inhibitors of these processes should prove useful in this endeavor.

Numerous inhibitors of amyloid formation have been discovered or designed; these include small molecules, peptides, and proteins that affect amyloid formation either by delaying the onset of fibril formation or diverting toxic aggregates to nontoxic aggregates with a different morphology. Most of the small molecule amyloidogenesis inhibitors are polyphenols that inhibit a wide variety of amyloidogenic sequences and fragments. In the case of (−)-epigallocatechin 3-gallate (EGCG), a green tea component, "inhibitory potency" against at least five diverse amyloidogenic systems has been demonstrated.[10,11]

Received: May 16, 2011
Revised: August 2, 2011
Published: August 17, 2011

It has been proposed that EGCG works by diverting poorly folded species to nonamyloidogenic oligomers and, eventually, nontoxic aggregates, rather than to amyloid fibrils via toxic preamyloid species.

Most of the peptide amyloidogenesis inhibitors presented in the literature are solubilized[12,13] and/or mutated versions[14] of the most amyloidogenic sequence fragments of the polypeptide system of interest. The common strategy is "β-assembly disruption" via introduction of residues that discourage β-strand formation and/or association such as proline, N-methylated, or α-disubstituted amino acid residues.[14−17]

A report by Ghosh and co-workers,[18] which demonstrated that a hyperstable mutant of the B1 domain of protein G could "evolve" into a potent inhibitor of aggregation of the Aβ(1−40) peptide, served to focus our attention on Trp and Tyr residues bearing β-hairpin peptides as potential amyloidogenesis inhibitors. The substitutions seen in the inhibitory protein included K → W, G → W, K → Y, and E → Y mutations. Seven of the eight mutations that appeared occurred on the exposed face of a single hairpin of the B1 domain. Over the past eight years, the a priori design of β-hairpins has been improved[19−23] to the point that 10−16-residue constructs that are >85% folded in water can be prepared routinely. As a result, we became interested in establishing whether designed β-hairpins could serve as minireceptors and pharmacophore display scaffolds for drug lead discovery.

We have previously reported that β-hairpin peptides bearing both Trp and Tyr residues inhibit fibril formation by human pancreatic amylin (hAM).[24] These inhibitory peptides bear no structural resemblance to hAM and expose Trp and Tyr residues at varying positions along the β-strands of the hairpin structure. The mechanistic hypothesis behind the use of these hairpins as inhibitors can be stated as follows: the prestructured strands of the β-hairpins bearing Trp and Tyr residues will facilitate intermolecular association and then sheet formation with preamyloid states and thus prevent or delay the self-self-recognition associated with β-oligomerization and fibril growth.

To probe the generality of our hypothesis regarding hairpin inhibition of amyloidogenesis, we tested a selection of aromatic-containing hairpins against another unstructured amyloidogenic system, α-synuclein (α-syn), using circular dichroism (CD), thioflavin T (ThT) fluorescence,[25,26] transmission electron microscopy (TEM) imaging, and Congo red (CR) staining: modulation of amyloidogenesis by β-hairpins was also observed for α-syn. We also confirm the inhibitory effect of our most potent Trp-containing hairpin inhibitor against hAM by TEM imaging, examine additional controls, and extend the study to cytotoxicity effects. These aromatic-containing hairpins are peptidic aggregation inhibitors that lack any sequence similarity with the amyloidogenic polypeptides yet appear to be among the most potent small peptide inhibitors of amyloidogenesis reported to date.

EXPERIMENTAL PROCEDURES

Materials. The α-synuclein sample was prepared at the University of Padova. Human α-synuclein cDNA was subcloned into the NcoI and XhoI restriction sites of the pET28a plasmid (Novagen). Because ~20% of the expression product from *Escherichia coli* represents mistranslation such that a cysteine residue is incorporated at position 136 instead of a tyrosine, site-directed mutagenesis of codon 136 (TAC to TAT) was employed. This results in the 100% expression of α-synuclein with the correct sequence. The protein was expressed in *E. coli* BL21(DE3) growing in Luria-Bertani medium. The overexpression product was recovered from the periplasm by osmotic shock as previously described.[27] The cell homogenate was boiled for 15 min, and the soluble fraction was treated with a two-step (35 and 55%) ammonium sulfate precipitation. The pellet was resuspended, dialyzed against 20 mM Tris-HCl (pH 8.0), loaded into a 6 mL Resource Q column (Amersham Biosciences), and eluted with a 0 to 500 mM NaCl gradient. After dialysis against Milli-Q water, the protein was lyophilized and stored at −20 °C.

For our preliminary studies, samples of hAM(1−37) remaining from prior studies[28] were repurified by high-performance liquid chromatography (HPLC) (C18). In addition, Amylin Pharmaceuticals provided two lots (25 and 10 mg) of hAM for the fibrillization inhibition studies. Synthetic hAM(1−37) obtained by Fmoc solid-phase peptide synthesis, as previously described,[29] was employed for the cytotoxicity studies.

Hexafluoro-2-propanol used in this study was a gift (lot 08012) from Halocarbon Corp., which is hereby acknowledged. All other solvents and chemicals used were reagent or spectroscopic grade commercial materials.

Peptide Synthesis. Peptide hairpins and controls were synthesized on an Applied Biosystems 433A peptide synthesizer using standard Fmoc solid-phase peptide synthesis methods. Wang resins preloaded with the C-terminal amino acid were employed. C-Terminal amides were prepared similarly but using Rink resins. Peptides were cleaved from the resin using a 95:2.5:2.5 trifluoroacetic acid (TFA)/triisopropylsilane/water mixture. The cleaved peptides were purified by reverse-phase HPLC on a Varian C18 prep-scale column using water/acetonitrile gradients (0.1 and 0.085% TFA). Collected fractions were lyophilized and their identity and molecular weight confirmed using a Bruker Esquire ion trap mass spectrometer.

NMR Spectroscopy. The derivation of NMR structures for bioactive peptides and controls was conducted using NOESY/TOCSY spectra as previously described.[21,22]

Aggregation and Aggregation Inhibition Assays. hAM assays were performed as previously described.[24] Stock solutions of hAM (400 μM) were prepared in neat HFIP and vortexed for 5 min. To initiate aggregation and/or fibril formation, the stock was diluted to 8 μM hAM with 5 mM phosphate buffer (pH 7.2), producing a final HFIP concentration of 2 vol %.

In the case of α-synuclein, we prepared 250 μL of 100 μM α-syn in 20 mM Tris-HCl buffer (pH 7.5) with 1.5 vol % HFIP in a vial containing a stir bar with or without added peptide inhibitors and/or ThT as follows. The ThT stock was a 800 μM solution in 20 mM Tris-HCl buffer (pH 7.5). Peptide inhibitor stocks were 1 mM solutions in the same buffer. The required amount of α-syn was placed in the 1 mL glass vial equipped with a small Teflon stir bar, to which were added either 200 μL of buffer or 150 μL of buffer and 50 μL of inhibitor stock (at 37 °C), and aggregation was initiated via addition of 50 μL of the HFIP stock solution. The HFIP stock was 7.5 vol % HFIP in 20 mM Tris-HCl buffer (pH 7.5). The process was conducted with continuous vigorous stirring; while the vial was incubated in a 37 °C water bath, aliquots were removed at different time points (every 2−3 h) for assays. To follow the time course of ThT signal development in controls and for inhibitors that resulted in accelerated cloudiness, 7 μL of the ThT stock was added just prior to HFIP addition and fluorescence measurements were taken at time zero and every 2−3 h thereafter as described below.

Circular Dichroism Spectroscopy. Stock peptide solutions for CD experiments were prepared in 10 mM phosphate buffer (or water/HFIP mixtures). The concentrations of the stock solutions were determined by the UV absorption of tyrosine and tryptophan (ε = 1190 and 5580 M^{-1} cm^{-1}, respectively, at 278 nm). CD samples with 6−30 μM peptide concentrations were prepared by dilution of the stock solution. Spectra were recorded on a Jasco J720 instrument in cells with a path length of 0.1 cm. Typical spectral accumulation parameters were as follows: scan rate of 100 nm/min with a 2 nm bandwidth and a 0.1 nm step resolution over the wavelength range of 185−270 nm with four to eight scans averaged for each spectrum. For time course experiments, this allows the collection of full spectral scans every 10 min. Raw ellipticity data were converted into molar, not residue-molar, ellipticity units (degrees square centimeters per decimole), using the Jasco software.

For CD experiments with α-syn aggregation samples, 5 μL aliquots of the assay sample (without added ThT) were removed and diluted with 195 μL of the 1.5% HFIP Tris-HCl buffer (final α-syn concentration of 2.5 μM). This was done every 2−4 h to monitor the transition from random coil to α-sheet signal. Correction for the CD contribution of the inhibitor is less significant but is used nonetheless.

ThT Fluorescence Detection of Amyloid Species. For α-syn aggregation assays, 200 μL of assay mixture was employed as described above. For assays that had been monitored by CD, 5 μL of the ThT stock was added 5 min prior to the fluorescence measurements, typically at the 16 h point in the assay.

Imaging Fibrils and Other Oligomers by Congo Red Staining and TEM. For TEM imaging, a 5 μL aliquot of a freshly agitated aggregation assay sample was adsorbed onto Formvar/carbon-coated 400 mesh copper grids and negatively stained with 2% uranyl acetate. Images were acquired using a Philips CM100 transmission electron microscope. For hAM assays, TEM images were typically obtained at 1, 2, 4, and/or 16 h. In the case of α-syn, images were obtained after 16−24 h.

The Congo red staining solution was prepared using to the method of Nilsson.[30] After incubation for 16−48 h, an aggregation assay mixture was agitated just prior to withdrawing a 10 μL sample that was placed onto a glass slide and air-dried, and 200 μL of Congo red solution was placed on the dried polypeptide sample. After a few minutes, the excess dye solution was blotted away and the sample observed in a light microscope (Olympus BX 60) equipped with crossed-polarized filters to observe birefringence.

Cell Viability Assays. Rat insulinoma cell line RIN5fm was employed; the cells were cultured and plated as previously described.[31] Freshly made solutions of hAM (5 μM) alone or mixtures of hAM (5 μM) with various amounts of WW2 or μPro1 as indicated were made in 10 mM sodium phosphate buffer (pH 7.4) containing 1% HFIP and incubated at room temperature for ∼20 h. Thereafter, the solutions were diluted with cell culture medium and added to the cells at the indicated final hAM concentrations. Following incubations with the cells for 20 h, cell damage was assessed by measuring the cellular reduction of MTT as previously described.[32] Of note, under the experimental conditions employed, hAM was in a nonfibrillar state at the beginning of the preincubation.[15]

RESULTS

Hairpin Peptides Examined as Modulators of Amyloidogenesis. The hairpins tested in this study were previously characterized by NMR and CD and are least 50% folded under the assay conditions. None of the hairpins or nonhairpin controls aggregated or enhanced thioflavin T (ThT) fluorescence, even at 2 mM after 5 days. The hairpins used in this study are shown in Scheme 1. The list includes controls as well as μPro1, a β-capped microprotein.[21]

Assay Conditions and Methods. Most previously reported α-syn aggregation assays have reported long lag times (days to many weeks) even at high protein concentrations (150−250 μM) with warming and aggressive agitation.[33,34] We chose to design an assay with a shorter lag time that would allow for ready monitoring of the course of amyloid formation by employing medium containing 1.5−2 vol % hexafluoro-2-propanol (HFIP). The incorporation of small amounts of HFIP is a common feature in many fibrillization assays.[34] The specific assay that we developed for hAM, 8 μM hAM in phosphate buffer (pH 7.2) containing 2 vol % HFIP, gave results consistent with the data of Miranker and co-workers.[35−37] The hAM fibrillization kinetics, as monitored by the ThT binding assay, were very similar to those from prior studies by

Scheme 1

A. Trp-, Tyr-pair bearing hairpin sequences [a,b]

Sequence	abbrev	class		citation
KKLTV**W**-I**p**GK-**W**ITVSA	WW2	MrH	(WloopW)	22
KKLTV**Y**-I**p**GK-**Y**ITVSA	YY2	MrH		22
KKLT**W**S-I**p**GK-K**W**TVSA	WW3	MrH		24
KKL**W**VS-I**p**GK-KI**W**VSA	WW4	MrH		22
C_2H_5CO-**W**-I**p**GK-**W**TG-NH_2	μPro1		(WloopW)	21
KT**W**-NAAAGK-**W**TE	HP7AAA	HP7	(WloopW)	
KAV**Y**-INGK-**W**TVE	HP6AYW		(YloopW)	22
B. Other hairpins and controls				
KK**Y**TVS-I**p**GK-KITVSA	MrH3b	MrH		60
Ac-KIVTSAK	ssMrH	"MrH"	single strand control	
KKLTV**W**I	ssW	"WW2"	single strand control	

[a]The peptide with no citation is analogous to the others of the same class (HP7),[20] prepared specifically for this study, and was synthesized and characterized by the methods given in the citation. [b]The peptides are classified by whether they have a Trp-flanked reversing loop[20,22] and whether they are derived from a hairpin originally based on the dimer interface of the Met repressor (MrH).[59,60] A bold lowercase p denotes D-Pro; aromatic residues are also highlighted in bold.

some of us.[15,31] The Raleigh group[38] has adopted a similar assay but with constant stirring that also accelerates aggregation. In the case of α-synuclein, the assay that gave reproducible aggregation time courses employed 100 μM α-syn, with addition of HFIP (to a final concentration of 1.5 vol %) to the stirred solution as the aggregation-initiating event. Munishkina[39] has also reported shorter lag times in buffers with added HFIP. For both amyloidogenic systems, lag times were measured using both CD spectroscopy and a ThT fluorescence assay. CR-stained and/or TEM images were obtained at the time corresponding to complete fibrillization in uninhibited assays (16 h for α-syn, 40−60 min for hAM) and at later time points.

hAM Aggregation Inhibition (TEM imaging confirms the CD and ThT assay results). Our previously reported results indicated that Trp-containing hairpins were among the more potent hairpins against hAM fibrillization.[24] The effects of selected hairpin peptides on hAM aggregation lag times appear in Table 1. The most potent inhibitor (WW2) is a Trp-flanked turn species; as a result, we added additional W-loop-W peptides to our screen. In light of the recent report[38] about the inhibition of hAM aggregation by rat amylin (rAM), we also included this nonamyloidogenic analogue as a "control" amylin-like species. The extent of inhibition observed [see also Table 3 (vide infra)] and the effects of selected hairpin peptides on hAM aggregation lag times appear in Table 1; representative time courses of ThT fluorescence in our assays appear in Figure 1.

In our assay, rAM was only a modest inhibitor requiring 6 molar equiv to effect a significant inhibition or display an increase in lag time. Of the additional W-loop-W peptides, one was essentially inactive and the other (μPro1) appeared to accelerate and enhance (an enhanced ThT signal) aggregation (see Figure 1). In a recent study, the Raleigh group[38] cautioned against relying on ThT fluorescence assays and employed TEM imaging for validation. In the case of the uninhibited assay, Figure 1b indicates that fibrils are indeed being formed. These fibrils are morphologically comparable to those in previously reported hAM studies with and without HFIP.[35,36,40] We chose our most active inhibitor (WW2, which increases the aggregation lag time by at least a factor of 3 when present in a 1-fold molar excess)[a] and the aggregation-enhancing μPro1 for TEM validation of hairpin effects on hAM aggregation (Figure 2) and cytotoxicity testing.

In the presence of 2 molar equiv of WW2, the hAM sample shows, in agreement with the CD and ThT assays,[24] no trace of fibrils after 2 h (Figure 2a). After 5 h, a few amorphous

Table 1. Hairpin Inhibition of hAM Aggregation[a]

	lag time[b] (min)			
peptide	1 molar equiv added	2 molar equiv added	4 molar equiv added	6 molar equiv added
rAM	50 (45−50)		50	93
MrH3b	–	–	55 (45)	65 (95)
WW2	151 ± 42 (167 ± 25)	253 ± 52 (120−300)	344 ± 28	–
WW3	(60)	(80)	98 ± 10 (180)	107 ± 33
WW4	(114)	82 ± 33 (105−120)	155 ± 11	333
YY2	139	201 ± 42 (70−80)	190	303 ± 37
YY3	–	58	52	44 (40)
other W-loop-W hairpins				
HP7AAA	–	70	–	–
μPro1	–	30 (35)	50	60

[a]The lag time for hAM aggregation is defined as the time at which the ThT signal reaches ∼15% of its final value and does vary [61 ± 14 min (n > 15)]; this also appears to be the point at which the CD β minimum (217 nm) in the CD spectrum becomes distinct (35−70 min). [b]Data for ThT with errors are from triplicate determinations; data from comparable CD assays are given in parentheses. The extreme sensitivity to the precise amount of HFIP is likely a source of lag time variability because it is difficult to control the HFIP content within 1.5 ± 0.1 vol % of the medium. Because the two measurements are always obtained in separate experiments, we do not know whether the measures are coincident in any specific run, but it appears that either can be used to monitor the aggregation time course.

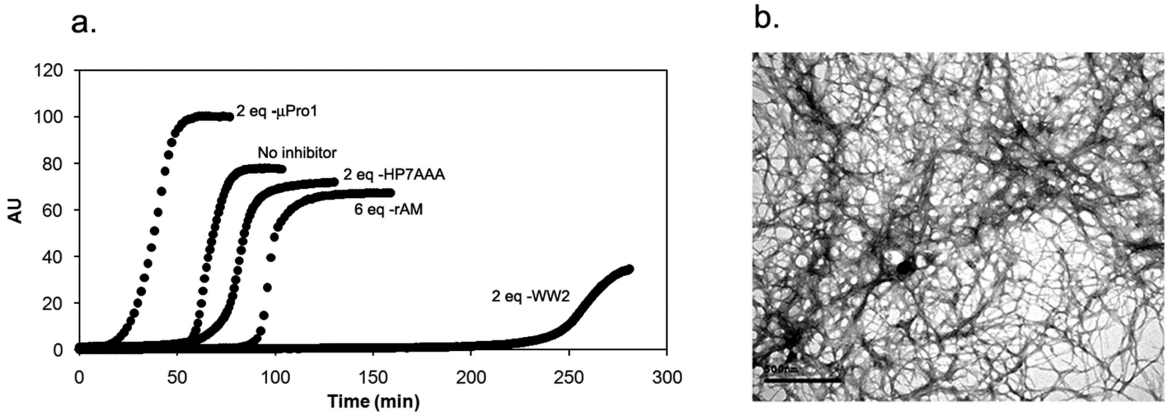

Figure 1. Human amylin aggregation assays. (a) Time course of ThT fluorescence development in a control and in the presence of selected peptides. (b) TEM image of hAM (uninhibited control) after 1 h. The scale bar represents 500 nm.

dx.doi.org/10.1021/bi200760h | Biochemistry 2011, 50, 8202−8212

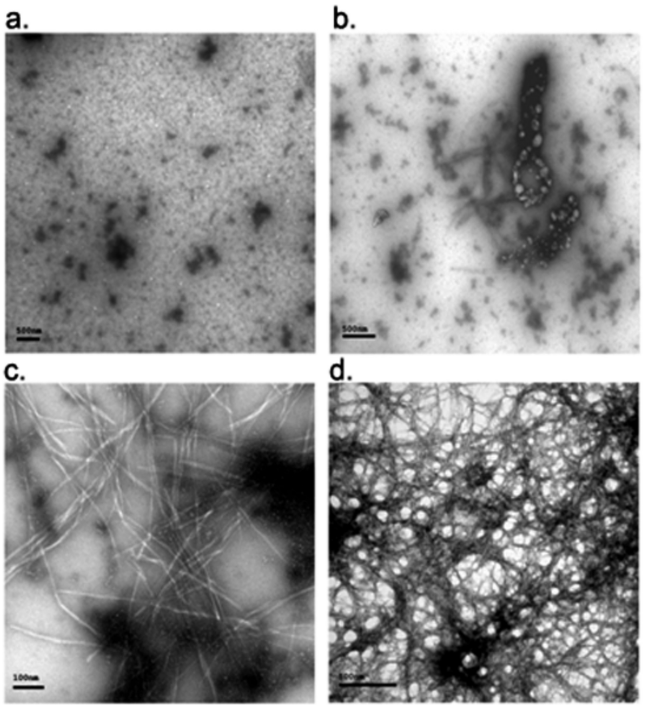

Figure 2. TEM images from hAM aggregation assays in the presence of Trp-bearing hairpin peptides. Panels a–c are representative panels from hAM with 2 molar equiv of WW2 at 2 (a), 5 (b), and 20 h (c). The scale bars for panels a, b, and d represent 500 nm; the scale bar for panel c represents 100 nm. Panel c was the grid displaying the greatest density of fibrils. Panel d was recorded after 40 min in the presence of 2 molar equiv of μPro1; a denser fibrillar network is observed at an early time point.

aggregates are observed (panel b), as well as occasional fibrils (none appear in most grids). After 20 h, some fibrils were found in most grids; panel c illustrates a particularly fibril-rich grid, but significant inhibition of fibril formation extended to the longest times examined. The TEM image of hAM in the presence of 2 molar equiv of μPro1 (Figure 2d) shows a denser web of fibrils after only 40 min. The fibril yield appears to be significantly greater than that observed for the uninhibited control after 60 min, which corroborates the results of the ThT and CD assays for this species (Table 1).

Inhibition of hAM Cytotoxicity. Inhibition of hAM fibrillogenesis has been previously shown to correlate with suppression of formation of cytotoxic hAM assemblies (e.g., ref 41). As a result, we sought to establish whether WW2 (the best of the hAM fibrillogenesis inhibitors identified here) would also suppress hAM cytotoxicity. For comparison, the effect of μPro1 on hAM cytotoxicity was also studied as this WW peptide has no inhibitory effect on hAM fibrillogenesis. For these studies, incubations of hAM and mixtures of hAM with WW2 or μPro1 aged for 24 h at different hAM:inhibitor molar ratios in 10 mM sodium phosphate buffer (1% HFIP) were added to RIN5fm cells (Figure 3). Following incubation for 20 h, cell viabilities were assessed by the MTT reduction assay. In the presence of 1 equiv of WW2, no inhibition of formation of cytotoxic assemblies was observed. However, a marked inhibition of hAM cytotoxicity was observed when a 2-fold excess of WW2 was applied that was consistent with the results of the ThT binding assay (Figures 1a and 2). A clear concentration dependence of the inhibitory effect of WW2 was found, with 6- and 10-fold excesses of this peptide strongly suppressing

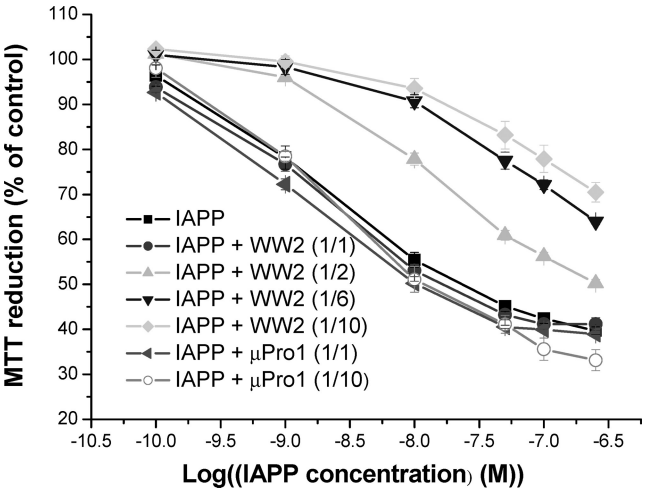

Figure 3. Effects of WW2 and μPro1 on cytotoxic self-assembly of hAM. Aliquots of incubations of hAM and mixtures of hAM with WW2 or μPro1 aged for 24 h at hAM:inhibitor molar ratios of 1:1, 1:2, 1:6, and 1:10 (in the case of WW2) and 1:1 or 1:10 (in the case of μPro1) in 10 mM sodium phoshate buffer (1% HFIP) were diluted with cell medium and added at the indicated final hAM concentrations to RIN5fm cells. Following incubation for 20 h, cell viabilities (% of control) were assessed by the MTT reduction assay. Data are means (±standard error of the mean) from three assays (n = 3 each).

formation of cytotoxic hAM assemblies (Figure 3). In contrast, no reduced hAM cytotoxicity was observed for hAM solutions containing μPro1 even at a 1:10 hAM:μPro1 molar ratio. These results were consistent with the results of the ThT assay and demonstrated that WW2, but not the control peptide (μPro1) with a similar Trp–Trp interaction geometry, when applied in a 2–10-fold molar excess over hAM, is able to either delay and suppress formation of cytotoxic assemblies derived from hAM or blunt their cytotoxic effect on rat insulinoma cells.

***α*-Synuclein Studies.** The α-syn species employed in our studies is the full-length 140-residue construct produced by overexpression in *E. coli* BL21(DE3) as described in Experimental Procedures. The top panels of Figure 4 illustrate α-syn aggregation as monitored by the CD and ThT assays. Uninhibited control solutions become somewhat cloudy 4–7 h[b] after HFIP addition (see Figure S1 of the Supporting Information); this is also the time point at which ThT fluorescence and the CD β-signature are in their growth phase. The aggregation of α-syn results in complete fibril formation over a 16 h time course. Amyloid fibril formation was also confirmed by CR staining (panels c and d) and TEM imaging (panel e). The α-syn fibrils produced in the 1.5% HFIP medium display morphology comparable to previous reports for media without cosolvent[33] and CR staining results in very bright apple-green birefringence, a hallmark of amyloid.[26,41]

We selected both potent and inactive hairpins from our study of hAM for screening in the α-syn aggregation assay. The inclusion of 2 molar equiv of potentially inhibiting peptides in α-syn fibrillization experiments resulted in a variety of responses (Table 2). Although modest delays in lag time as assayed by CD were observed in some cases, the more common observation was an earlier cloud point or immediate precipitation of nonamyloid aggregates. Even MrH3b, with only a single aromatic residue, which had no effect on hAM aggregation, produced accelerated precipitation. Other MrH hairpin sequences (data not shown), even ones with greatly

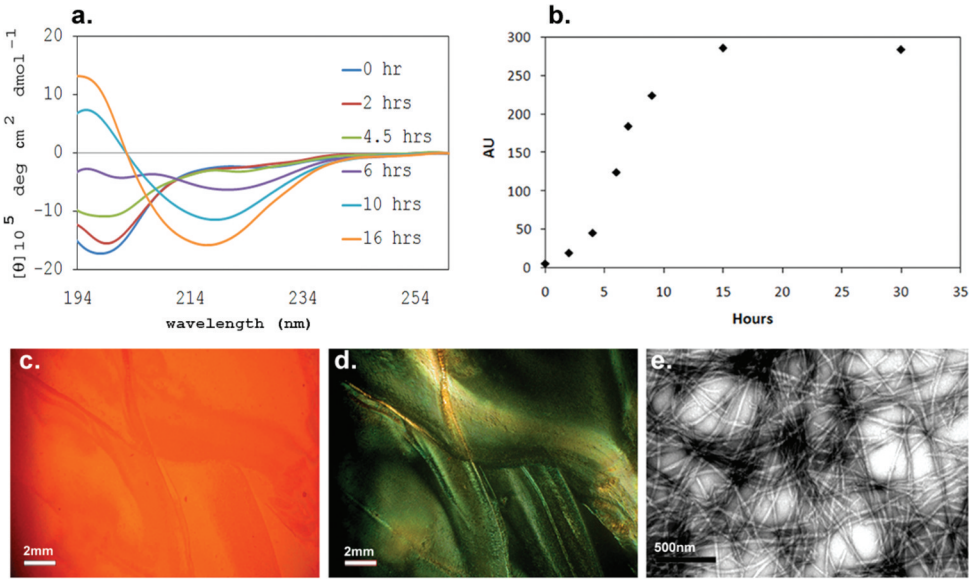

Figure 4. (a) CD molar ellipticity vs wavelength and (b) ThT assays monitoring α-syn aggregation over a period of 16−30 h. The bottom panels illustrate CR-stained images (at 48 h) under nonpolarized (c) and polarized (d) light; bright green birefringence is shown in panel d (the scale bars represent 2 mm). A TEM image of the α-syn assay after incubation for 16 h is shown in panel e (the scale bar represents 500 nm).

Table 2. Effects of Added Peptides on α-syn Aggregation and Fibril Formation

peptide inhibitor	visible cloudiness	β CD signal	ThT Fl[a] (%)	fibril morphology[b]	Congo red staining[c]
WW2	immediate	not applicable	19 ± 5	short thick fibrils with AA	little/no BiR
WW3	immediate	not applicable	20	short thick fibrils	not determined
YY2	immediate	not applicable	18 ± 7	spherical aggregates	little/no BiR
MrH3b	within 1 h	CD intensity implies parts per trillion, 10% β	32 ± 7	not determined	not determined
HP6AYW	slight after 4−6 h	β signal within 6 h, 93% at 16 h	93 ± 12	normal	bright green BiR[c]
μPro1	slight after 8 h	β signal delayed, but 100% β at 16 h	69 ± 9	normal	green BiR[c]
HP7AAA	after 7 h	delayed but full β signal appears (100% at 16 h)	81 ± 10		
4 equiv	delayed	delayed (84% β at 16 h, 100% β on day 3)	67	normal morphology and yield at 5 days	
		Nonhairpin Controls			
ssMrH	slight after 4−6 h	β signal within 6 h, 100% at 16 h	≥90	normal	not determined
ssW	after 6 h	helical at 4−6 h, 80% β at 16 h	61 ± 7	normal with AA	some/green BiR[c]

[a]ThT fluorescence is reported as the percentage of the uninhibited control value at 16 h and is given with the experimental error for triplicate experiments. Typical measurements at time zero were 5−26 AU units. A >11-fold enhancement in fluorescence at 482 nm is observed upon fibril formation. The control ThT fluorescence value at 16 h was well reproduced, 291 ± 9 AU. [b]AA designates amorphous aggregates. [c]Congo red staining leads to bright green birefringence (BiR) for amyloid species.

reduced hairpin populations, also displayed some acceleration of precipitation. When the MrH hairpins bearing two aromatic side chains were present, immediate cloudiness was observed upon HFIP addition.[b] CD data could not be collected for the α-syn assay solution containing these hairpins because the aggregates that formed reduced the observed CD intensities and precluded accurate determination of the CD difference spectrum. The cloudiness that appears 4−7 h after initiation with α-syn alone or in the presence of peptides that do not affect the lag time did not have this effect: reproducible CD difference spectra could be generated after HFIP addition for at least 20 h. The enhancement of ThT fluorescence at 16 h was strongly inhibited by hairpins that produced immediate cloudiness.

In contrast, a hairpin with shorter strands (HP6AYW) but retaining a biaryl-flanked turn was essentially inactive (see Figure S2 of the Supporting Information). Peptides μPro1 and HP7AAA have even shorter β-strand segments. HP7AAA, a stable hairpin with an EtF W−W interaction, displayed dose-dependent inhibition: the β-CD signal development was still incomplete after 48 h at a 4:1 molar ratio (inhibitor:α-syn) (see Table 2). After 5 days, fibrils with the control morphology are present as determined by TEM. Peptide μPro1 was also modestly inhibiting with no evidence of accelerated precipitation.

The precipitation phenomenon, not observed in the hAM studies, led us to use CR staining as an additional assay. Although this assay is not quantitative, it does visualize and characterize the aggregates formed. Because the complete assay mixture, dispersed by agitation just prior to slide preparation, is assayed, precipitation does not present problems in the TEM imaging and CR staining assays. Representative images for WW2- and YY2-inhibited runs appear in Figure 5. According to TEM and CR staining, few, if any, fibrils with the normal morphology were observed for α-syn in the presence of WW2 and YY2. Rather, WW2 produced thicker

dx.doi.org/10.1021/bi200760h | Biochemistry 2011, 50, 8202−8212

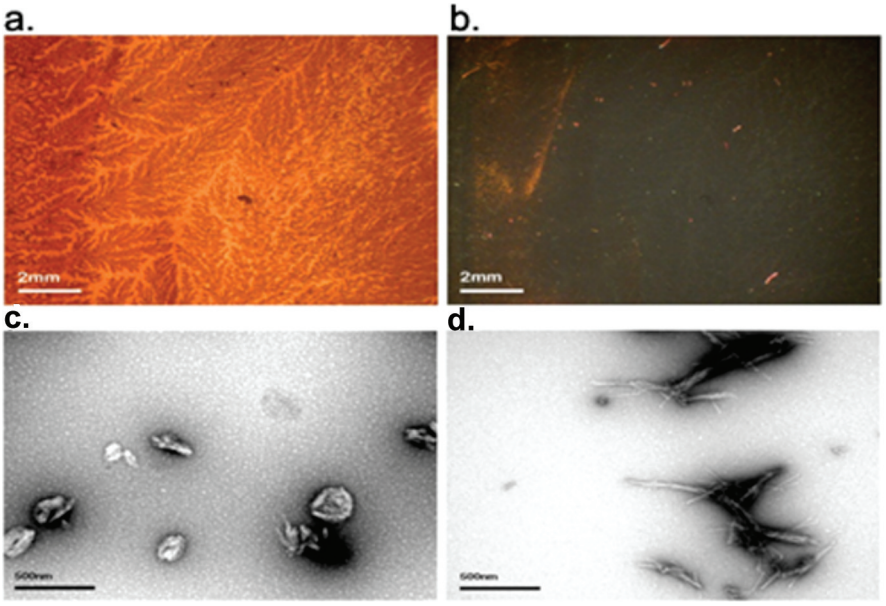

Figure 5. CR staining and TEM images of α-syn in the presence of β-hairpin peptides. Panels a and b illustrate CR staining images with and without polarized light, respectively, for α-syn aggregation in the presence of 2 molar equiv of YY2. TEM images of α-syn with 2 molar equiv of YY2 (c) and WW2 (d) are also shown. Congo red images of WW2 are almost identical to those seen for YY2 (data not shown).

short fibrils, while YY2 resulted in what appears to be spherical aggregates. For both "inhibitors", CR staining was less extensive, and no trace of bright green birefringence was observed (see Figure 5).

Control Peptides. Two specific single-strand controls for hairpins (ssMrH and ssW) were included in our study. Ac-KIVTSAK (ssMrH) represents one strand of MrH3b, and KKLTVWI (ssW) serves as the single-strand control for the WW2 series of hairpin peptides. Like a number of short peptides tested (data not shown), ssMrH had no effects on the course of α-syn aggregation. However, ssW (the Trp-containing control) delays aggregation (as monitored by CD) and displayed a significant reduction in ThT fluorescence at the 16 h read time. Unlike noninhibited control assays, which shift cleanly from random coil to β by CD, in the presence of ssW, a helical CD spectrum (minima at 207 and 222 nm) is present at the 4 and 6 h points in the assay (Figure 6).

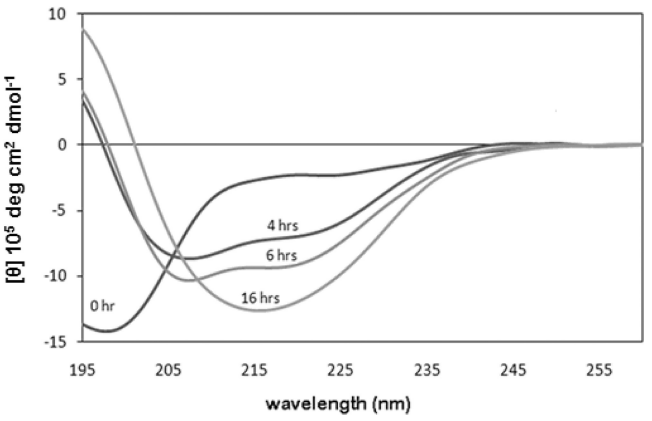

Figure 6. CD difference spectra recorded for α-syn in the presence of peptide ssW and 1.5 vol % HFIP. The ellipticity $[\theta]$ scale is in molar not residue molar units. The zero time point is immediately after HFIP addition.

DISCUSSION

The two amyloidogenic systems examined in this study (hAM and α-syn), although having no sequence similarities, are both random coil peptides that convert to amyloid fibrils over a period of days at the concentrations examined in the aqueous buffers employed. Including 1.5−2 vol % HFIP in the assay buffer resulted in complete amyloid formation over a period of hours rather than days. Under these conditions, lag times were reproducible as was the extent of ThT fluorescence enhancement observed. The TEM images and CR staining characteristics of the amyloid fibrils produced correspond to those observed in the absence of HFIP by other researchers. This is also the case for the amplitude of the β-CD signal that is observed.[c]

Our previous report on hAM inhibition indicated that stable MrH hairpins with aromatic side chains at non-H-bonded sites were effective at retarding β-structure formation (CD) and delaying fibril formation. Inhibition of hAM aggregation was observed as a dose-dependent increase in the lag time for amyloid nucleation coupled, in most cases, with a decreased yield of fibrils as quantitated by ThT fluorescence[24] (see also Figure 1). The decreased yield of fibrils has now been confirmed by TEM (Figure 2), which also verifies the aggregation acceleration and enhancement produced by μPro1. Rat amylin (rAM) has recently[38] been reported as an effective inhibitor of WT hAM amyloid formation, though prior reports[15] indicated that rAM does not significantly inhibit the formation of cytotoxic hAM aggregates. Hairpins WW2, YY2, and WW4 are significantly more potent than rAM in our assay. Control peptides, including hairpins lacking aromatic residues, and at least one stable hairpin with a W-loop-W unit (HP7AAA) had no significant effect on hAM aggregation. A summary of the observed effects of added hairpins on amyloid fibril formation assays for both hAM and α-syn appears in Table 3.

A mechanistic rationale that includes the original basis for these studies, hairpin association with a preamyloid patch retarding self-self-recognition, and can be used to discuss the

Table 3. Summary of the Effects of the Hairpin Peptide on hAM and Synuclein Amyloid Formation[a]

hairpin peptide	hAM[b]	synuclein[c]
WW2	<5%[d]	19 ± 5%
	4-fold extended lag phase[d]	a few fibrils with alternate
	inhibits cytotoxicity	nonamyloid (CR) aggregate precipitation
WW3	80 −100%	20%
	slight delay in onset at 6 equiv	fibrils with alternate morphology
YY2	42 ± 6%	18 ± 7%
	delayed onset[e]	spherical aggregates
		nonamyloid (CR) aggregate precipitation
MrH3b	no effect even at 4 equiv	32%
μPro1	123 ± 7%	69%
	shorter lag phase, greater yield of fibrils by TEM, no effect on hAM cytotoxicity	normal fibril morphology and staining morphology
HP7AAA	90%	80%
	no effects, confirmed by TEM	slight delay at onset

[a]The ThT fluorescence (as a percentage of the uninhibited control) observed with 2 molar equiv of added hairpin appears as the first entry, followed by other observations for each species. [b]ThT fluorescence measured at 2.5 h. The full reference response is observed at 1.2 h for uninhibited controls with little or no loss in signal over the next 2 h. [c]ThT fluorescence measured at 16 h for α-syn assays. CR refers to Congo red staining and the observation of birefringence. [d]The ThT fluorescence measured at 5 h was 43% of that observed in a control. [e]A 5-fold extension of the lag phase is observed when 6 equiv of YY2 is added to hAM, with modest levels of ThT fluorescence observed only after 5 h.

results appears in Figure 7. In Figure 7, the course of hAM amyloid fibril formation is modeled after the recent report by Zanni and co-workers[42] and incorporates the fibril cross-section geometry of Luca et al.[43] The preamyloid conformation can be viewed as a partially formed β-arch.[44] According to Shim et al.,[42] the hAM oligomerization process begins near the HSSNN reversing loop of the β-arch. The asterisk on the initiating, partially formed β-arch indicates a hydrophobic site, which includes V17, the site that achieves a $^{13}C{=}^{18}O$ coupled β-state earlier than any other in oligomerization studies of hAM isotopomers.[42] We view inhibitor binding at such a site as the initial driving force for complex formation with β-sheet formation serving to mask the self-self-recognition region required for oligomerization. This model predicts the dose-dependent increase in the lag time that is observed. Given that cytotoxicity is generally attributed to oligomers,[7−9] the observation of hAM cytotoxicity inhibition by peptide WW2 supports the hypothesis that the hairpins bind to a preamyloid state. It has been established[15] that hAM is in a nonfibrillar state at the beginning of the preincubation used in the cytotoxicity assay. In the uninhibited preincubations of hAM, both fibril and cytotoxic assemblies form, with significant rat insulinoma cell toxicity evident at concentrations as low as 1 nM (Figure 3). Two molar equivalents of peptide WW2 provides nearly complete protection from this cytoxic challenge.

While the specific model is based on hAM, the general features are likely to apply to other amyloidogenic systems, as well. In the case of α-syn, there are several suspect amyloidogenic patches[12,45] with hydrophobic binding sites in the NAC region. However, the preamyloid conformation is likely to be a more complex superpleated β-structure.[44] The alternative pathway to nonamyloid aggregates was added to Figure 7 because this mechanism is suggested for α-syn amyloid fibril inhibition.

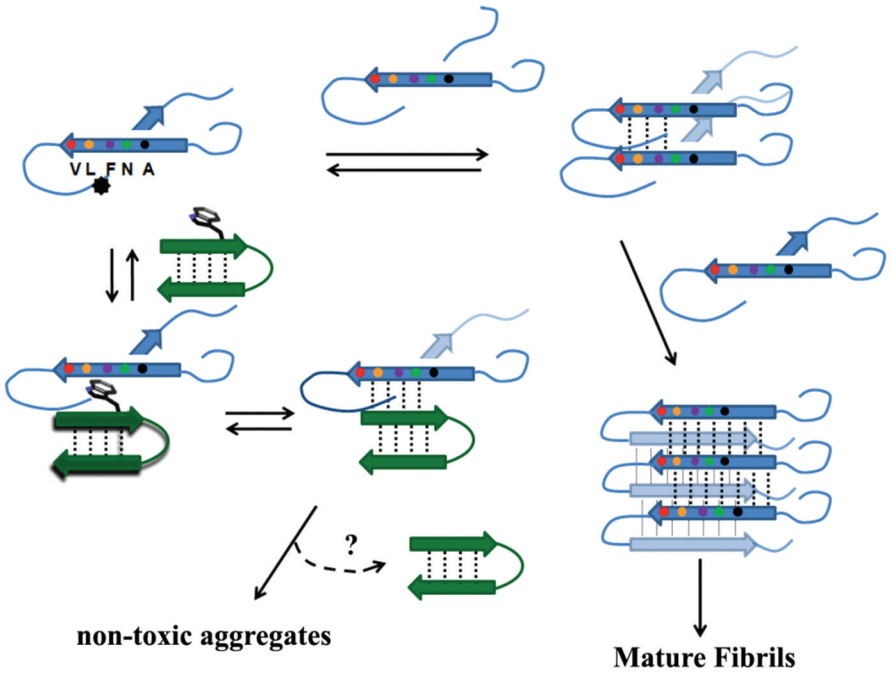

Figure 7. Mechanistic model for the inhibition of amyloid formation by a hairpin bearing an exposed hydrophobic site (shown as a tryptophan side chain). The β-arch geometry of the preamyloid state is modeled after the proposal of Shim et al.[42] for hAM aggregation. The asterisk on the starting structure indicates a hydrophobic binding site. The alternative route, the formation of nonamyloid aggregates, is included to extend the model to α-syn, for which this pathway appears to be the dominant one in the presence of the hairpin examined in this study.

dx.doi.org/10.1021/bi200760h | Biochemistry 2011, 50, 8202–8212

The course of α-syn amyloidogenesis was more sensitive to hairpin structures. To date, all hairpin peptides with five-residue β-strands, even those with less stable folds, have resulted in some inhibition as assessed by ThT fluorescence at 16 h. The interpretation of the ThT assay data has a potential caveat: the weakened signal may reflect the formation of aggregates that have precipitated and are thus not observed in the fluorimetric assay. As a result, we rely to a greater extent on visual inspection (appearance of precipitates), TEM, and CR-stained imaging of the complete assay mixtures for the analyses. For peptides WW2, WW3, and YY2, TEM imaging indicated either no fibrils or a greatly reduced yield of fibrils of abnormal morphology. These assay mixtures displayed weakened CR staining with little or no green birefringence. The common feature of these inhibitors was immediate or accelerated (vs noninhibited controls) cloudiness and the production and precipitation of amorphous aggregates. In the case of peptides WW2 and YY2, amorphous aggregates were also observed in the absence of added HFIP. Whether these nonamyloid aggregates contain the added hairpin peptides has not been determined to date; Figure 7 recognizes both possibilities.

In one case (with peptide YY2 present), we observed what appear to be spherical aggregates (Figure 5). Tubular and annular structures, designated as protofibrils, have been the subject of significant study.[12,46−48] However, the protofibrils reported are much smaller (10−24 nm in diameter) than the structures seen in our case (160−260 nm in diameter); 70−90 nm diameter annular oligomers have been observed for α-syn under quite different conditions, with their formation accelerated in the presence of 100 μM Ca^{2+} ions.[47] We view the larger spherical species observed in the presence of YY2 as off-path, nonamyloidogenic aggregates resulting from the diversion of a preamyloid state present at a low equilibrium concentration from the onset to an alternative aggregation pathway. This mechanism of amyloidogenesis inhibition has been suggested for EGCG, a polyphenol that also affords spherical aggregates with α-syn,[10] that has high-profile citations as a potential therapeutic strategy.[7] We observe nonamyloid precipitates of α-syn with as little as 0.5 molar equiv of peptide WW2; the similar effect with EGCG requires a 5-fold excess of the "inhibitor". A similar diversion of a preamyloid state has also been observed with IAPP-GI, a designed hAM mimic:[15] we also found spherical oligomers and suggested the sequestration of hAM and Aβ from their cytotoxic self-association pathways in the form of nonfibrillar heterocomplexes with IAPP-GI.[29]

Stable hairpins retaining similar W/W pairs (e.g., μPro1 and HP7AAA), but with shorter β-strands, appear to have diminished inhibitory activity for both amyloid systems. In the case of hAM, μPro1 was the only species to accelerate aggregation and afford an increased yield of fibrils (Figure 2d) while HP7AAA had no significant effects on hAM aggregation. Consistent with this observation, μPro1 had no effect on hAM-induced cytotoxicity (Figure 3). In the case of α-syn, μPro1 had, if any effect, a slight lag time prolongation. HP7AAA consistently prolonged the α-syn lag time. While further screening, including other classes of hairpins, will be needed for a confirmation, our tentative conclusion is that a minimum β-strand length is required to compete with the oligomerization that leads to α-syn fibril growth.

CD assays of amyloid formation for both hAM and α-syn imply, with one exception, a direct conversion of a random coil signal to a β-structure signal with no observable intermediate state. The exception was the observation of a helical signal for α-syn at intermediate times in the presence of a control peptide (ssW) that corresponds to a single strand of an active hairpin inhibitor (Figure 6). Helix conformations have recently been implicated in the fibril formation pathways for Aβ and hAM.[49,50] α-syn has been reported to favor helix formation in SDS-containing and organic solvent media.[51−53] Some reports note that membrane surfaces can accelerate α-syn fibrillization;[54] others,[55] however, suggest that lipid binding and helical conformations result in fibrillization inhibition. Because we never observed helical features in CD spectra recorded at intermediate times for noninhibited α-syn control assays, we attribute the helical CD signals observed at intermediate points when the ssW peptide is present to oligomerization inhibition that allows the observation of a helical preamyloid state.

These studies suggest that aromatic residue display is involved in the initial formation of preamyloid−inhibitor complexes, but this is, in the case of α-syn, not sufficient to prevent self-self-recognition. In the case of hAM, the aromatic moieties play a deciding role; the exposed β-strand edges of hairpins are not sufficient for establishing inhibitory interactions with hAM amyloidogenesis intermediates. The MrH hairpins with multiple aromatic residues are, in both systems, amyloid formation inhibitors. They are mostly effective when the hairpins include Trp residues. This observation is not that surprising given that Trp residues are often observed at peptide−protein interfaces,[56] form favorable cross-strand interactions in β-sheet systems, and occur frequently in prior peptide modulators of amyloidogenesis.[18,57,58]

In our case, we have demonstrated both cross-reactivity with hAM and α-syn and the inhibition of hAM-induced cytotoxicity by a hairpin peptide that bears no similarity in sequence to either amyloidogenic system. Whether designed hairpins can serve as leads for therapeutic development remains to be determined; however, the modulation of amyloidogenesis pathways by these hairpins should provide probes for NMR studies of the early stages of the processes by adjusting conditions under which the lag time of the noninhibited assay may be further delayed to allow for NMR measurements. We anticipate that formation of the preamyloid−inhibitor complex will occur in the absence of added HFIP and that these complexes will have sufficient lifetimes for NMR characterization to provide both insights into the biorecognition phenomena along the pathway to cytotoxic assemblies and guidance for the design of more effective inhibitors that could serve as leads for therapeutic development.

■ ASSOCIATED CONTENT

Ⓢ Supporting Information

Effect of precipitation of hairpin peptides on α-syn aggregation as well as TEM and CR images of an additional control hairpin peptide in the presence of α-syn. This material is available free of charge via the Internet at http://pubs.acs.org.

■ AUTHOR INFORMATION

Corresponding Author

*E-mail: andersen@chem.washington.edu. Telephone: (206) 543-7099. Fax: (206) 685-8665.

Funding

Funding from the National Science Foundation (CHE0650318) and the National Institutes of Health (3R01-GM059658-08S1).

■ ACKNOWLEDGMENTS

NMR studies were conducted on instruments that were purchased or upgraded from facility grants from the National Institutes of Health and the National Science Foundation. TEM training was provided by W. Chan (Department of Biology, University of Washington), and images were collected at the Biology Imaging Facility at the University of Washington. Congo red images were taken with a polarized light microscope provided by the Electron Microscopy Center at the University of Washington. We thank J. Bernhagen (RWTH Aachen University) for help with the cell viability assays.

■ ABBREVIATIONS

hAM, human amylin; MTT, 3-(4,5-dimethylthiazol-2-yl)-2,5-diphenyltetrazolium bromide; rAM, rat amylin; TEM, transmission electron microscopy; ThT, thioflavin T; CR, Congo red.

■ ADDITIONAL NOTES

[a]With 4 molar equiv of WW2, the lag time increases to 5.7 h (a 5-fold increase), and ∼50% inhibition of the ThT fluorescence signal is still observed at 7 h.[24]

[b]In the absence of addition of HFIP, α-syn solutions remain fully transparent for many days. When aromatic-bearing hairpins that result in immediate α-syn precipitation upon addition of HFIP are added to α-syn in the absence of HFIP, immediate precipitation is not observed. The solutions do become cloudy over a period of hours: 2 h for 2 molar equiv of peptide WW2 and 4−6 h for the same conditions with YY2. For both peptides, precipitation occurs immediately upon adjustment of the medium to an HFIP content of 1.5 vol %. In the case of WW2/α-syn mixtures, nonamyloid precipitates are obtained with as few as 0.5 equiv of the added peptide. It is apparent that the interaction of α-syn with these peptides favors aggregate formation, and that this process, like amyloidogenesis, is greatly accelerated by the presence of 1.5 vol % HFIP. Control experiments show that the hairpin conformational equilibrium is not altered upon addition of these low levels of HFIP cosolvent.

[c]Our prior study of β CD characteristics[61] can be used to estimate the fractional contributions of β-strand conformations in the fibril states. The mature fibril[49] $[\theta]_{216}$ values for hAM ranged from −16000° to −20000°, indicating that virtually all of the residues are in β-strand conformations in the fibril state. Similar values have been reported for hAM aggregation studies in media without added cosolvents.[40,62] The minimum β for α-syn in our assay corresponds to −11300°/residue, in excellent agreement with values reported by other laboratories[26,33] for assays conducted in the absence of cosolvents. This ellipticity value implies that ca. 60% of the synuclein sequence is in β-strand conformations in the fibril state.

■ REFERENCES

(1) Chiti, F., and Dobson, C. M. (2009) Amyloid formation by globular proteins under native conditions. *Nat. Chem. Biol. 5*, 15−22.

(2) Cooper, G. J., Willis, A. C., Clark, A., Turner, R. C., Sim, R. B., and Reid, K. B. (1987) Purification and characterization of a peptide from amyloid-rich pancreases of type 2 diabetic patients. *Proc. Natl. Acad. Sci. U.S.A. 84*, 8628−8632.

(3) Goedert, M. (2001) α-Synuclein and neurodegenerative diseases. *Nat. Rev. Neurosci. 2*, 492−501.

(4) Ferrone, F. (1999) Analysis of protein aggregation kinetics. *Methods Enzymol. 309*, 256−274.

(5) Ruschak, A. M., and Miranker, A. D. (2007) Fiber-dependent amyloid formation as catalysis of an existing reaction pathway. *Proc. Natl. Acad. Sci. U.S.A. 104*, 12341−12346.

(6) Lansbury, P.T. (1997) Inhibition of amyloid formation: A strategy to delay the onset of Alzheimer's disease. *Curr. Opin. Chem. Biol. 1*, 260−267.

(7) Roberts, B. E., and Shorter, J. (2008) Escaping amyloid fate. *Nat. Struct. Mol. Biol. 15*, 544−546.

(8) Haass, C., and Selkoe, D. J. (2007) Soluble protein oligomers in neurodegeneration: Lessons from the Alzheimer's amyloid β-peptide. *Nat. Rev. Mol. Cell Biol. 8*, 101−112.

(9) Haataja, L., Gurlo., T., Huang, C. J., and Butler, P. C. (2008) Islet amyloid in type 2 diabetes, and the toxic oligomer hypothesis. *Endocr. Rev. 29*, 303−316.

(10) Ehrnhoefer, D. E., Bieschke, J., Boeddrich, A., Herbst, M., Masino, L., Lurz, R., Engemann, S., Pastire, A., and Wanker, E. E. (2008) EGCG redirects amyloidogenic polypeptides into unsctructured, off-pathway oligomers. *Nat. Struct. Mol. Biol. 15*, 558−566.

(11) Hudson, S. A., Ecroyd, H., Dehle, F. C., Musgrave, I. F., and Carver, J. A. (2009) (−)-Epigallocatechin-3-Gallate (EGCG) Maintains κ-Casein in its pre-fibrillar state without redirecting its aggregation pathway. *J. Mol. Biol. 392*, 689−700.

(12) El-Agnaf, O.M. A., Paleologou, K. E., Greer, B., Abogrein, A. M., King, J. E., Salem, S. A., Fullwood, N. J., Benson, F. E., Hewitt, R., Ford, K. J., Martin, F. L., Harriott, P., Cookson, M. R., and Allsop, D. (2004) A strategy for designing inhibitos of α-synuclein aggregation and toxicity as a novel treatment for Parkinson's disease and related disorders. *FASEB J. 18*, 1315−1317.

(13) Austen, B. M., Paleologou, K. E., Ali, S. A. E., Qureshi, M. M., Allsop, D., and El-Agnaf, O. M. A. (2008) Designing peptide inhibitors for oligomerization and toxicity of Alzheimer's β-amyloid peptide. *Biochemistry 47*, 1984−1992.

(14) Kapurniotu, A., Schmauder, A., and Tenidis, K. (2002) Structure-based design and study of nonamyloidogenic, double N-methylated IAPP amyloid core sequences as inhibitors of IAPP amyloid formation and cytotoxicity. *J. Mol. Biol. 315*, 339−350.

(15) Yan, L.-M., Tararek-Nossol, M., Velkova, A., Kazantzis, A., and Kapumiotu, A. (2006) Design of a mimic of nonamyloidogenic and bioactive human islet amyloid polypeptide (IAPP) as nanomolar affinity of IAPP cytotoxic fibrillogenesis. *Proc. Natl. Acad. Sci. U.S.A. 103*, 2046−2051.

(16) Gilead, S., and Gazit, E. (2004) Inhibition of amyloid fibril formation by peptide analogues modified with α-aminoisobutyric acid. *Angew. Chem., Int. Ed. 43*, 4041−4044.

(17) Etienne, M.A., Aucoin, J. P., Fu, Y., McCarley, R. L., and Hammer, R. P. (2006) Stoichiometric inhibition of amyloid β-protein aggregation with peptides containing alternating α,α-disubstituted amino acids. *J. Am. Chem. Soc. 128*, 3522−3523.

(18) Smith, T. J., Stains, C. I., Meyer, S. C., and Ghosh, I. (2006) Inhibition of β-amyloid fibrillization by directed evolution of a β-sheet presenting miniature protein. *J. Am. Chem. Soc. 128*, 14456−14457.

(19) Cochran, A. G., Skelton, N. J., and Starovasnik, M. A. (2001) Tryptophan zippers: Stable, monomeric β-hairpins. *Proc. Natl. Acad. Sci. U.S.A. 98*, 5578−5583.

(20) Andersen, N. H., Olsen, K. A., Fesinmeyer, R. M., Tan, X., Hudson, F. M., Eidenschink, L. A., and Farazi, S. R. (2006) Minimization and optimization of designed β-hairpin folds. *J. Am. Chem. Soc. 128*, 6101−6110.

(21) Kier, B. L., and Andersen, N. H. (2008) Probing the lower size limit for protein-like fold stability: Ten-residue microproteins with specific, rigid structures in water. *J. Am. Chem. Soc. 130*, 14675−14683.

(22) Eidenschink, L. A., Kier, B. L., Huggins, K. N. L., and Andersen, N. H. (2009) Very short peptides with stable folds: Building on the interrelationship of Trp/Trp, Trp/cation, and Trp/backbone-amide interaction geometries. *Proteins: Struct., Funct., Bioinf. 75*, 308−322.

(23) Kier, B. L., Shu, I., Eidenschink, L. A., and Andersen, N. H. (2010) Stabilizing capping motif for β-hairpins and sheets. *Proc. Natl. Acad. Sci. U.S.A. 107*, 10466−10471.

(24) Huggins, K. N. L. Andersen, N. H. (2010) Hairpin peptide inhibitors of amyloid fibril formation. In *Chemistry of Peptides in Life Science, Technology and Medicine* (Lankinen, H., Ed.) Peptides 2008 (Proceedings of the 30th European Peptide Symposium) pp 590−591.
(25) Naiki, H., Higuchi, K., Hosokawa, M., and Takeda, T. (1989) Fluorometric determination of amyloid fibrils in vitro using the fluorescent dye, thioflavine T. *Anal. Biochem. 177*, 244−249.
(26) Conway, K.A., Harper, J. D., and Lansbury, P. T. (2000) Fibrils formed in vitro from α-synuclein and two mutant forms linked to Parkinson's disease are typical amyloid. *Biochemistry 39*, 2552−2563.
(27) Huang, C., Ren, G., Zhou, H., and Wang, C.-C. (2005) A new method for purification of recombinant human α-synuclein in *Escherichia coli*. *Protein Expression Purif. 42*, 173−177.
(28) Cort, J. R., Liu, Z., Lee, G. M., Huggins, K. N. L., Janes, S., Prickett, K., and Andersen, N. H. (2009) Solution state structures of human pancreatic amylin and pramlintide. *Protein Eng., Des. Sel. 22*, 497−513.
(29) Yan, L.-M., Velkova, A., Tatarek-Nossol, M., Andreetto, E., and Kapurniotu, A. (2007) Designed IAPP Mimic Blocks Aβ Cytotoxic Self-Assembly: Cross-Suppression of Amyloid Toxicity of Aβ and IAPP Suggests a Molecular Link between Alzheimer's Disease and Type 2 Diabetes. *Angew. Chem., Int. Ed. 46*, 1246−1252.
(30) Nilsson, M. R. (2004) Techniques to study amyloid fibril formation in vitro. *Methods 34*, 151−160.
(31) Tatarek-Nossol, M., Yan, L. M., Schmauder, A., Tenidis, K., Westermark, G., and Kapurniotu, A. (2005) Inhibition of hIAPP amyloid-fibril formation and apoptotic cell death by a designed hIAPP amyloid-core-containing hexapeptide. *Chem. Biol. 12*, 797−809.
(32) Tenidis, K., Waldner, M., Bernhagen, J., Fischle, W., Bergmann, M., Weber, M., Merkle, M. L., Voelter, W., Brinner, H., and Kapurniotu, A. (2000) Identification of a penta- and hexapeptide of islet amyloid polypeptide (IAPP) with amyloidogenic and cytotoxic properties. *J. Mol. Biol. 295*, 1055−1071.
(33) Hoyer, W., Antony, T., Cherny, D., Heim, G., Jovin, T. M., and Subramaniam, V. (2002) Dependence of α-synuclein aggregate morphology on solution conditions. *J. Mol. Biol. 322*, 383−393.
(34) Fink, A. L. (2006) The aggregation and fibrillation of α-synuclein. *Acc. Chem. Res. 39*, 628−634.
(35) Miranker, A. D., and Padrick, S. B. (2001) Islet amyloid polypeptide: Identification of long-range contacts and local order on the fibrillogenesis pathway. *J. Mol. Biol. 308*, 783−794.
(36) Padrick, S. B., and Miranker, A. D. (2002) Islet amyloid: Phase partitioning and secondary nucleation are central to the mechanism of fibrillogenesis. *Biochemistry 41*, 4694−4703.
(37) Koo, B. W., and Miranker, A. D. (2005) Contribution of the intrinsic disulfide to the assembly mechanism of islet amyloid. *Protein Sci. 14*, 231−239.
(38) Cao, P., Meng, F., Abedini, A., and Raleigh, D. P. (2010) The ability of rodent islet amyloid polypeptide to inhibit amyloid formation by human islet amyloid polypeptide has important implications for the mechanism of amyloid formation and the design of inhibitors. *Biochemistry 49*, 872−881.
(39) Munishkina, L. A., Phelan, C., Uversy, V. N., and Fink, A. L. (2003) Conformational behaviour and aggregation of α-synuclein in organic solvents: Modeling the effects of membranes. *Biochemistry 42*, 2720−2730.
(40) Goldsbury, C., Goldie, K., Pellaud, J., Seeling, J., Frey, P., Muller, S. A., Kistler, J., Cooper, J. S., and Aebi, U. (2000) Amyloid fibril formation from full-length and fragments of amylin. *J. Struct. Biol. 130*, 352−362.
(41) Puchtler, H., Sweat, F., and Levine, M. (1962) On the binding of congo red by amyloid. *J. Histochem. Cytochem. 10*, 355−364.
(42) Shim, S.-H., Gupta, R., Ling, Y. L., Strasfeld, D. B., Raleigh, D. P., and Zanni, M. T. (2009) Two-dimensional IR spectroscopy and isotope labeling defines the pathway of amyloid formation with residue-specific resolution. *Proc. Natl. Acad. Sci. U.S.A. 106*, 6614−6619.
(43) Luca, S., Yau, W. M., Leapman, R., and Tycko, R. (2007) Peptide conformation and supramolacular organization in amylin fibrils: Constraints from solid-state NMR. *Biochemistry 46*, 13505−13522.
(44) Kajava, A. V., Baxam, U., and Stevem, A. C. (2010) β arcades: Recurring motifs in naturally occurring and disease-related amyloid fibrils. *FASEB J. 24*, 1311−1319.
(45) Du, H.-N., Li, H.-T., Zhang, F., Lin, X.-J., Shi, J. H., Shi, Y.-H., Ji, L.-N., Hu, J., Lin, D.-H., and Hu, H.-Y. (2006) Acceleration of α-synuclein aggregation by homologous peptides. *FEBS Lett. 580*, 3657−3664.
(46) Lashuel, H. A., Petre, B. M., Wall, J., Simon, M., Nowak, R. J., Walz, T., and Lansbury, P. T. Jr. (2002) α-Synuclein, especially the Parkinson's disease-associated mutants, forms pore-like annular and tubular protofibrils. *J. Mol. Biol. 322*, 1089−1102.
(47) Lowe, R., Pountney, D. L., Jensen, H. P., Gair, W. P., and Voelcker, N. H. (2004) Calcium(II) selectively induces α-synuclein annular oligomers via interaction with the C-terminal domain. *Protein Sci. 13*, 3245−3252.
(48) Rochet, J.-C., Conway, K. A., and Lansbury, P. T. (2000) Inhibition of fibrillization and accumulation of prefibrillar oligomers in mixtures of human and mouse α-synuclein. *Biochemistry 39*, 10619−10626.
(49) Abedini, A., and Raleigh, D. P. (2009) A critical assessment of the role of helical intermediates in amyloid formation by natively unfolded proteins and polypeptides. *Protein Eng., Des. Sel. 22*, 453−459.
(50) Williamson, J. A., Loria, J. P., and Miranker, A. D. (2009) Helix stabilization precedes aqueous and bilayer-catalyzed fiber formation in islet amyloid polypeptide. *J. Mol. Biol. 393*, 383−396.
(51) Bisaglia, M., Tessari, I., Pinato, L., Bellanda, M., Giraudo, S., Fasano, M., Bergantino, E., Bubacco, L., and Mammi, S. (2005) A topological model of the interaction between α-synuclein and sodium dodecyl sulfate micelles. *Biochemistry 44*, 329−339.
(52) Bisaglia, M., Trolio, A., Bellanda, M., Bergantino, E., Bubacco, L., and Mammi, S. (2006) Structure and topology of human α-synuclein bound to micelles: Implications for the aggregation process. *Protein Sci. 15*, 1408−1416.
(53) Munishkina, L. A., Henriques, J., Uversky, V. N., and Fink, A. L. (2004) Role of protein-water interactions and electrostatics in α-synuclein fibril formation. *Biochemistry 43*, 3289−3300.
(54) Lee, H. J., Choi, C., and Lee, S. J. (2002) Membrane-bound α-synuclein has a high aggregation propensity and the ability to seed the aggregation of the cytosolic form. *J. Biol. Chem. 277*, 671−678.
(55) Zhu, M., and Fink, A. L. (2003) Lipid Binding Inhibits α-Synuclein Fibril Formation. *J. Biol. Chem. 278*, 16873−16877.
(56) Ma, B., Elkayam, T., Wolfson, H., and Nussinov, R. (2003) Protein-protein interactions: Structurally conserved residues distinguish between binding sites and exposed protein surfaces. *Proc. Natl. Acad. Sci. U.S.A. 100*, 5772−5777.
(57) Sato, T., Kienlen-Campard, P., Ahmed, M., Liu, W., Li, H., Elliott, J. I., Aimoto, S., Constantinescu, S. N., Octave, J.-N., and Smith, S. O. (2006) Inhibitors of amyloid toxicity based on β-sheet packing of Aβ40 and Aβ42. *Biochemistry 45*, 5503−5516.
(58) Nagai, Y., Inui, T., Popiel, H. A., Fujikake, N., Hasegawa, K., Urade, Y., Goto, Y., Naiki, H., and Toda, T. (2007) A toxic monomeric conformer of the polyglutamine protein. *Nat. Struct. Mol. Biol. 14*, 332−340.
(59) Maynard, A. J., Sharman, G. J., and Searle, M. S. (1998) Origin of β-hairpin stability in solution: Structural and thermodynamic analysis of the folding of model peptide supports hydrophobic stabilization in water. *J. Am. Chem. Soc. 120*, 1996−2007.
(60) Dyer, R. B., Maness, S. J., Franzen, S., Fesinmeyer, R. M., Olsen, K. A., and Andersen, N. H. (2005) Hairpin Folding Dynamics: The cold-denatured state is predisposed for rapid refolding. *Biochemistry 44*, 10406−10415.
(61) Cort, J. R., et al. (1994) β-Structure in human amylin and two designer β-peptides: CD and NMR spectroscopic comparisons suggest soluble β-oligomers and the absence of significant populations of β-strand dimers. *Biochem. Biophys. Res. Commun. 204*, 1088−1095.
(62) Porat, Y., Mazor, Y., Efrat, S., and Gazit, E. (2004) Inhibition of islet amyloid polypeptide fibril formation: A potential role for heteroaromatic interactions. *Biochemistry 43*, 14454−14462.